8th Biennial International Conference
& Exposition on Petroleum Geophysics

"HYDERABAD 2010"

P-326

Electrical signatures of the shallow crustal features across the NSL zone using magnetotelluric study, central India

G. Dhanunjaya Naidu and T. Harinarayana*** *National Geophysical Research Institute*

Summary

Magnetotelluric (MT) study is carried out across the NSL zone along a 190 km long N-S trending traverse extends from Balapur in the South to Andharwadi in the North. As a part of the study we have collected 14 magnetotelluric soundings and data were rotated to N70^0 E after removing the local distortions arising from the 3D galvanic effects using Groom- Bailey decomposition technique. Bostick 1-D (rotationally invariant) inversion has been carried out in order to add value to the 2-D inversion results. 2D inversion has been carried out by using NLCG scheme and the results are compared with seismic study. The derived results gave the thickness of the alluvial cover, trap, sediments and depth to the basement and its variation all along the traverse.

The 1D and 2D modeling results for shallow crustal section has brought out a moderately resistive layer (50-200 Ωm) representing the exposed volcanic rock cover, followed by a layer of 20-100 Ωm inferred to be subtrappean sediments underlined by the high resistive (> 1000 Ohm-m) basement. The Deccan trap thickness varies from around a few tens of meters to a maximum of 1.5 km along the traverse. A subtrappean sedimentary basin like feature is delineated in the middle of the traverse with a thickness amounting to as much as 2 km. The basement is very shallow (few tens of meters) on northern side of the traverse, it becomes deep in the middle of the traverse and its thinning as we go towards south.

Key words: magnetotellurics; shallow crust; Nramda-Tapti region; electrical conductivity

1. Introduction

The Narmada-Son lineament (NSL) is oriented in E-W/ENE-WSW direction crosses the central Indian region. Geologically, the Narmada valley can be divided into two parts: one towards the western part of Barwaha, where the river bed and the valley passes through deccan traps, and towards the east of Barwaha, the valley all along exposes older hard rocks comprising of the Upper Vindhyan sediments of late Precambrian age, the older Bijawar sediments, Archean phyllites, quartzites and granitoid rocks (Gosh, 1976). Origin of the Narmada valley is considered to be formed in two distinctly different periods: after commencement of the eruption of Deccan trap, and the period prior to it. From various geological studies, it is close to the zone of fractures belonging to early Precambrian, Cretaceous and post Deccan trap period. The present valley dates back predominantly to the pre-Deccan trap period. Although its tectonic movements began significantly before Deccan traps it still continues to a certain extent. The pre-trappean topography is visible at places, where the basalts have been eroded. Evidence of sedimentation along this zone is reported in the Jurassic period. Deccan traps belonging to late Cretaceous to early Paleocene (Wellman and Mc Elhinny, 1970). Deccan traps, towards south and north of the lineament, have been dated from 66 Ma to about 64 Ma (Alexander, 1981) respectively.

Many views have been provided regarding tectonic setting of the lineament. West (1962) stated that the Narmada-Son line appears to be a zone of weakness from Precambrian times with the areas to the north and south moving up and down relative to each other and noted that Gondwana rocks are exposed to the south and Vindhyan rocks are exposed to the north of NSL. According to Agarwal and Gaur (1972), an E-W rift, 70 km wide, is extending along the Narmada-Tapti system. Ahmed (1964) considered NSL as a swell in the crust. Qureshy (1964) described this feature as a horst, delimited by Son-Narmada fault on the northern side and Tapti fault to the south. Mall et al., (2005) have identified

*dhanugeo@yahoo.co.in

the faults as weak zones, where hot springs also emerges at places and described that they are the sources for seismically active regions. The study area consists of various geological, tectonic features and major lineaments (Fig.1).

Integrated geophysical studies with gravity, magnetic, deep electrical resistivity methods during CRUMANSONATA (1995) program have been carried out (Rao et al., 1982; Rao and Sastry, 1986) and during Upper mantle project (Kailasam, 1979) to understand the crust and upper mantle structure of NSL particularly in respect of density and velocity structures. Singh and Meissner (1995) noticed high density underplated layer at the base of the crust beneath the Narmada-Tapti region. Apart from gravity, five deep seismic sounding (DSS) traverses also carried out across NSL and the results have shown anomalous crustal structure with a velocity range of 7.0-7.5 km/s (Kaila et al., 1985). Although these studies have provided valuable information, imaging through deep electromagnetic methods provides additional information on the nature of the deep crustal signatures. The tectonic processes, the crust mantle interactions and partial melting conditions in this region, can be understood more clearly from deep electromagnetic study. Earlier magnetotelluric (MT) study results (Harinarayana et al., 2007 and Patro et al., 2005) found a moderately conductive (50-500 Ohm-m) features from mid to lower crustal depths with high density (2.95 gm/cc) and high seismic velocity (7-7.2 km/s) and magmatic under plating of the crust is inferred. Magma emplacement from deeper levels to magmatic under plating of the crust is inferred. Magma emplacement from deeper levels to upper-lower crustal depths was also reported in the study region (Rao et al., 2004). In order to add value to these results and also to the earlier DSS, gravity, deep electrical and deep electromagnetic studies, MT measurements have been initiated. It is assumed to study the nature of the crust and mantle structure and to examine the electrical signatures of the known faults like Narmada South Fault-NSF, Tapti Fault-TF, Gavilgarh Fault-GF and Purna Fault-PF. Present traverse is N-S trending with a length of 190 km along Andharwadi (A) – Balapur (B) crossing all the major E-W/ENE-WSW faults like NSF, TF, GF and PF. The traverse also cuts across the Satpura gravity high and covers mostly in the region of exposed Deccan traps at the middle of the traverse. High resistive shelf facies cover towards the northern part and alluvial deposits to the southern part near Purna River. Since present MT traverse passes close to the DSS line from Ujjain to Mahan, the present MT study results are integrated with DSS along with regional gravity results.

2. Data analysis

The data for the present study are acquired during 2005-06. A total of 14 sites are occupied along the N-S trending traverse. The *ADU-06 (Analog Digital Unit),* the core unit of the multi-channel Geophysical Measurement System of M/s Metronix, Germany has been used for MT data recording in the frequency range of 1000-1/1000 Hz. The two horizontal electric field measurements perpendicular to each other (e.g., north and east) is measured using lead-lead chloride electrodes of Wolf Chemical Limited, Hungary. The magnetic fields are measured with MFS-06 (M/s Metronix) induction coil magnetometers.

All the data are analyzed using Mapros software (M/s Metronix, Germany). In order to obtain MT impedance tensor and magnetic transfer functions, robust single-station processing to down-weight or discard outliers of impedance estimates is used at each frequency band of measurement (Sutarno and Vozoff, 1989; Vozoff and Jupp, 1997). Initially the time series are edited manually by removing bad segments contaminated by noise (e.g. spikes). The remaining data are transformed from time domain to frequency domain using FFT algorithm. Cross-correlations between Hx-Ey and Hy-Ex pairs are computed; spectra are smoothed and stacked for impedance estimation. Because of the logistic constrains, we could not acquire the remote reference (RR) data and is not used in data processing. Data quality is good for majority of the stations except for some of the stations at higher frequencies due to cultural noise. Unfortunately, the Hz data quality is poor for majority of the stations. Hence, Hz data is not used for analysis and induction arrows are not shown. Examples of measured impedance tensor components are shown in figure 2.

In order to obtain the strike angle free from near surface distortions, the impedance tensors at each site for all frequencies are decomposed using Groom Bailey decomposition scheme (Groom and Bailey, 1989). The impedance tensors for all frequencies at each site are rotated at intervals of 5^0 to obtain the shear and twist for each rotation. This determines the frequency invariant values of the shear and twist and also the range of the strike

angles over which these parameters are reasonably stable. The derived shear and twist values at each site are fixed and the unconstrained strike angles are obtained at each frequency for all the sites. Strike has a weak dependence on the twist and shear and thus such large variations are not unusual. The regional strike found in the range of N55^0 E and N80 E for the frequencies (100-0.001 Hz) of all the sites and a strike of N70^{0}E is observed to be the best-fitting. This suggests a regional strike direction of N70^{0}E as most of the sites are in the close vicinity of the major tectonic elements oriented in the same direction. In an earlier study of the nearby MT traverse, located parallel to the present traverse, N 75^{0}E is obtained as the geoelectric strike (Patro et al., 2005). Thus the derived geoelectric strike from the data is consistent with the established regional geological strike of the faults and also with the earlier studies in the same region. The impedance tensors for all the frequencies and sites are rotated along this direction with the shear and twist constrained. The apparent resistivity and phase along this direction are assigned to be TE-mode (parallel to the strike) and perpendicular to it as TM-mode (perpendicular to the strike).

3. 2D inversion results

The 2-D inversion has been done using the Rodi and Mackie's (2001) RLM2DI code. This finds regularized solutions (Tikhonov Regularization) to the two-dimensional inverse problem for MT data using the method of non-linear conjugate gradients (NLCG) to minimize an objective function that penalizes data residuals and second spatial derivatives of resistivity. The inversion parameter is a uniform grid Laplacian which assumes for the purposes of computing the regularization function that the dimensions of the model are all equal and produce a smooth model. Here the Laplacian $(\nabla^2 m)^2$ is minimized. This solves the inverse problem in the sense of Tikhonov and Arsenin (1977), taking a "regularized solution" to be a model minimizing an objective function 'Ψ' for a given λ, V, and L defined by

$$\Psi(m) = (d - F(m))^T V^{-1} (d - F(m)) + \lambda m^T L^T L m$$

The regularization parameter, λ, is a positive number. The positive-definite matrix V plays the role of variance of error vector 'e'. The second term of Ψ defines a stabilizing function on the model space. In this study, we choose the matrix L to be a simple, second-difference operator such that, when the grid of model block is uniform, Lm approximates the Laplacian of log ρ.

It may lead to artifacts, if vertical and horizontal grid spacings are significantly different. Therefore, grid spacing is kept as uniform as possible within the region of interest. The MT responses along the strike (TE-mode) and orthogonal to the strike (TM-mode) are jointly considered for inversion to obtain geo-electric model along the traverse.

The behavior of the inversion process is mainly controlled by a trade-off parameter "*t*" representing a measure of compromise between data fit and model smoothness. Higher value of this parameter leads to smooth model but data fit may not be good, where as lower value leads to good data fit but model smoothness may not be good. The inversion is also repeated with different resistivity values of 50, 100, 500 and 1000 Ohm-m for the uniform half space as initial model and the inversion with 100 Ohm-m, the model seems to be appropriate as the apparent resistivity for the highest frequency of measurement asymptotic to this value for most of the sites. An error floor of 20% for apparent resistivity and 5% (1.5^0) for phase is assigned, thus downweighing the apparent resistivity with respect to phase. This in turn helps minimizing the static shift effect in apparent resistivities. This will also yield better data fit for phase while there may be small deviations in apparent resistivity. The horizontal smoothing factor a = 5 is used for the inversion. Root mean square (RMS) error parameter is taken as the misfit between the observed and modeled data. Here the value of the misfit is 2.1% for the derived model after 100 iterations. Beyond 80 iterations, the RMS misfit remained constant. The derived 2-D model is presented in figure. 3 and discussed under shallow geoelectric crustal section.

4. Shallow geoelectric crustal section

Shallow geoelectric section (0-4 km) is presented in figure 3. Surface geological features such as alluvium near Purna River at the sites N15 and O16 towards southern end of the traverse can be seen with a maximum thickness of about 400m lie over a moderately resistive layer (300 m) Followed by sedimentary formations (500 m) and high resistive basement. In order to delineate the subsurface section more clearly for shallow depths, 1-D inversion has also been carried out for all the stations in order to add

value to the 2-D inversion. An example of Bostick 1-D layer modeling results for the rotationally invariant response shows moderately resistive layer, sediments and basement depths for the selected 2 stations G16 and J16 (Fig.4). The moderately resistive layer thickness increases from 300 m towards south increases gradually to about 1.5 km near NSF close to the stations F16 and G16 (Fig.3). About 2 km thick sub-trapean sediments (30-50 Ω m) near NSF and TF gradually thinning (500m) towards south. The depth to the resistive (> 1000 Ω m) basement is about 3.5 km near NSF and becomes shallow to 1.5 km towards south. The basement depth sharply decreases from 3.5 km to 250 m near station E16, north of NSF. Such a sharp change in the basement structure is indicative that NSF plays a major role for the deposition of subtrapean sediments in the NSL region. Such a sharp change near NSF has also been indicated from an earlier DSS study (Kaila et al., 1985) located about 40 km west of the present traverse.

5. Discussion of the results

The results derived from the present study is compared and discussed in the following with the earlier DSS results.

Since our traverse passes close to the earlier DSS (Kaila et al., 1985) along Ujjain-Mahan profile, the 2D geoelectric section is also compared with the seismic section (Fig.3 top). However, as our traverse is limited to Narmada river towards north and Balapur towards south (near Mahan of DSS profile), the geoelectric section is compared with Dorwa-Mahan part of the seismic section. As can be seen from the figure that the basement depth derived from our study closely matches with the DSS results. Additionally, sharp variation of resistivity structure in the form of a fault derived from geoelectric section near the station F16 (near NSF) is well mapped in DSS shallow section also.

The study region is seismically active as two major earthquakes – Satpura (M6.3, 1938) at a depth of 40 km and Jabalpur earthquake (M6.0, 1997) at a depth of 30 km have occurred. Reactivation of deep seated faults and variation of local stress concentration are believed to be the causative mechanism for the seismicity (Campbell, 1978; Sykes 1978; Coward, 1994). The occurrence of deep focus earthquakes (30-40 km) is an indication that deep seated faults are related to crust mantle interaction. The variation in the thickness of high resistive thick upper crust towards north and middle (20 – 30 km) and thin towards south (15 km) indicated from our study may be an additional factor to increase the stress concentration in NSL region.

6. Conclusions

The geoelectric section derived from 2D inversion of the magnetotelluric data has shown the basement faults clearly demarcated with sharp resistivity variation near Narmada south fault with a sharp depth variation extending from 0.25 km to as deep as 3.5 km. This feature is also indicated from DSS. Trap thickness is about 300 m towards south gently increases to about 1.5 km near NSF. The subtrappean sediment thickness is 2 km near NSF and gradually reduces to half a kilometer towards south. The resistivity contrast between the sediments and basement seen to be well resolved but not so prominent between the trap and the sediments.

The presence of alluvium is clearly seen as high conductive feature near Gavilgarh and Purna faults with a maximum thickness of about 400 m. The subtrappean sediments at places have exhibited in the form of high conductive features from 2D modeling study due to data gaps.
These features need to be mapped more clearly with close station interval at these locations.

Acknowledgements

We wish to thank Dr.V.P.Dimri, Director, N.G.R.I. for permitting to publish this work. We also would like to thank Dr.R.S.Sastry, Dr.K.Veeraswamy and Sri.D.N.Murthy for useful discussions and all the help regarding modeling work. Help rendered by Sri Arvind Kumar Gupta in drafting the figures on the computer is greatly appreciated. G.Dhanunjaya Naidu thanks CSIR for the Senior Research Fellowship.

References

Agarwal, P.N. and Gaur, V.K., 1972. Study of crustal deformation in India. Tectonophysics. 15, 287-296.

Ahmed, F., 1964. The line of Narmada-Son Valley. Curr.Sci. 33, 362-363.

Alexander, P.O., 1981. Age and duration of Deccan trap volcanism: K-Ar evidence in Deccan Volcanism edited by K.V.Subba Rao and R.N.Sukheswala. Mem.Geol.Soc.Ind. 3, 244-258.

Campbell, D. L., 1978. Investigation of the stress-concentration mechanism for intraplate earthquakes. Geophys. Res. Lett. 5, 477–479.

Coward, M., 1994. Inversion tectonics. In Continental Deformation (ed. Hancock, P. L.), Pergamon Press, Amsterdam. 289–304.

CRUMANSONATA, 1995. Geoscientific studies of the Son-Narmada-Tapti Lineament Zone. Geological Survey of India, special publication. 10, 158, 244.

Gosh, D. B., 1976. The nature of Narmada-Son Lineament. In Seminar volume on tectonics and Metallurgy of South and East Asia. Misc. Publ Geol. Surv. Ind. 34,119–132.

Groom, R.W. and Bailey, R.C., 1989. Decomposition of magnetotelluric impedance tensor in the presence of local three-dimensional galvanic distortion. J.Geophys.Res. 94, 1913-1925.

Hansen, P.C., 1998. Rank Deficient and Discrete Ill-Posed Problems, Numerical Aspects of Linear Inversion. SIAM, Philadelphia.

Harinarayana, T., Patro, B.P.K., Veeraswamy, K., Manoj, C., Naganjaneyulu, K., Murthy, D.N. and Virupakshi, G., 2007. Regional Geoelectric structure beneath Deccan volcanic province of the Indian subcontinent using magnetotellurics. Tectonophysics. 445, 66–80.

Kaila, K.L., Reddy, P.R., Dixit, M.M., Koteswar Rao, P., 1985. Crustal structure across the Narmada–Son lineament, Central India from deep seismic soundings. J. Geol. Soc. India. 26, 465–480.

Kailasam, L.N., 1979. Plateau uplift in peninsular India. Tectonophysics 61, 243-269 . Mall, D.M., Singh, A.P., Sarkar, D., 2005. Structure and tectonics of satpura, central India. Curr. sci. 88 , 10, 1621-1627.

Patro, B.P.K., Harinarayana, T., Sastry R.S.,Madhusushana Rao., Manoj C., Naganjaneyulu K., Sarma. S.V.S., 2005. Electrical imaging of Narmada-Son Lineament Zone, Central India from magnetotellurics. Physics of the Earth and Planetary Interiors. 48, 215-232.

Qureshy, M. N., 1964. Gravity anomalies as related to regional tectonics of Peninsular India. Rep. 22nd Int. Geol.Congr., New Delhi, Part IV, 490-506.

Rao, C.K., Ogawa, Y., Gokarn, S.G., Gupta, G., 2004. Electromagnetic imaging of magma across the Narmada Son lineament, central India. Earth Planets Space. 56, 229–238.

Rao, A.P., Venkateswarulu, P.D., Rao, K.J., Kamaraju, M.V.V., 1982. Report on the geophysical investigations under CRUMANSONATA project in the Bagh area, Dhar district, M.P. Unpublished Progress Report of the GSI for FS, 79–80.

Rao, K.V., and Sastry, P.R., 1986. A geophysical investigation along Kanti- Nagpur traverses under project CRUMANSONTATA. Unpublished Report GSI, CR.

Rodi, W. and Mackie, R.L., 2001. Nonlinear conjugate gradients algorithm for 2D magnetotelluric inversions. Geophysics. 66, 174–187.

Seismotectonic atlas of India and its environs, 2000. Geological survey of India.

Singh, A.P. and Meissner, R., 1995. Crustal configuration of the Narmada-Tapti region (India) from gravity studies. J. Geodynamics. 20, 111-127.

Sutarno, D. and Vozoff, K., 1989. Robust M-estimation of magnetotelluric impedance tensors. Explor. Geophys. 20, 383–398.

Sykes, L.R., 1978. Intra-plate seismicity, reactivation of pre-existing zones of weakness, alkaline magmatism and other tectonism postdating continental fragmentation. Rev. Geophys. 16, 621–688.

Tikhonov, A. N. and Arsenin, V. Y., 1977. Solutions of ill-posed problems. Winston, V. H. and Sons. Washington, D.C.

Vozoff, K. and Jupp, D.L.B., 1997. The magnetotelluric methods in the exploration of sedimentary basins-discussion. Geophysics. 62(2), 692–692.

Wellman, P. and Mc Elhinny, M.W., 1970. K-Ar age of the Deccan traps, India. Nature. 227 595-596.

West, W.D., 1962. The line of Narmada–Son Valley. Curr. Sci. 31, 43–144.

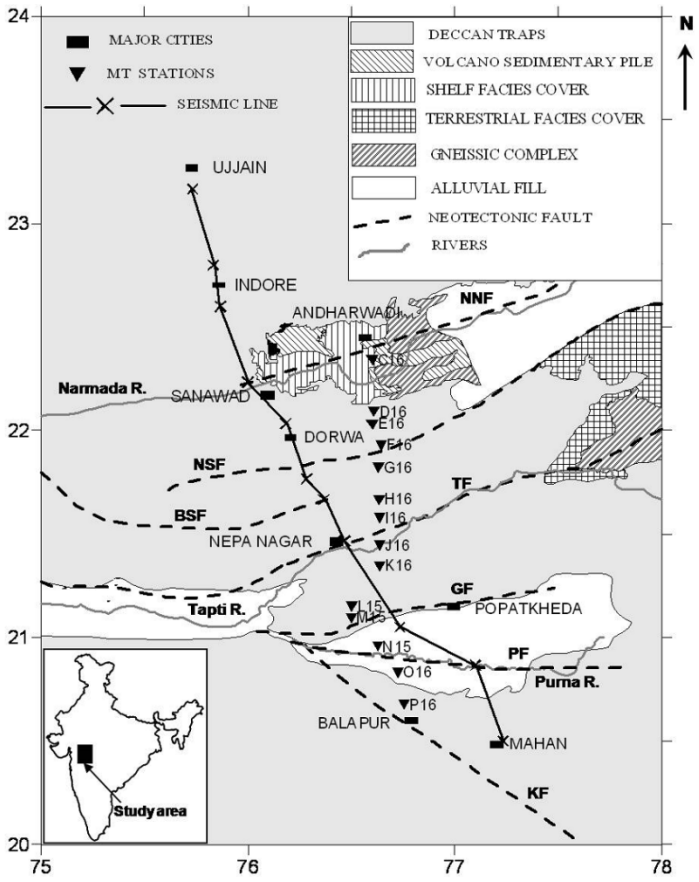

Fig.1. Location of the Andharwadi-Balapur-AB traverse (MT soundings are black triangles) plotted on geological and tectonic map of the present study area. (From GSI). Cross and black line is the DSS profile along Ujjain-Mahan. Dashed lines indicate the prominent geological faults. (Seismotectonic atlas of India. 2000)

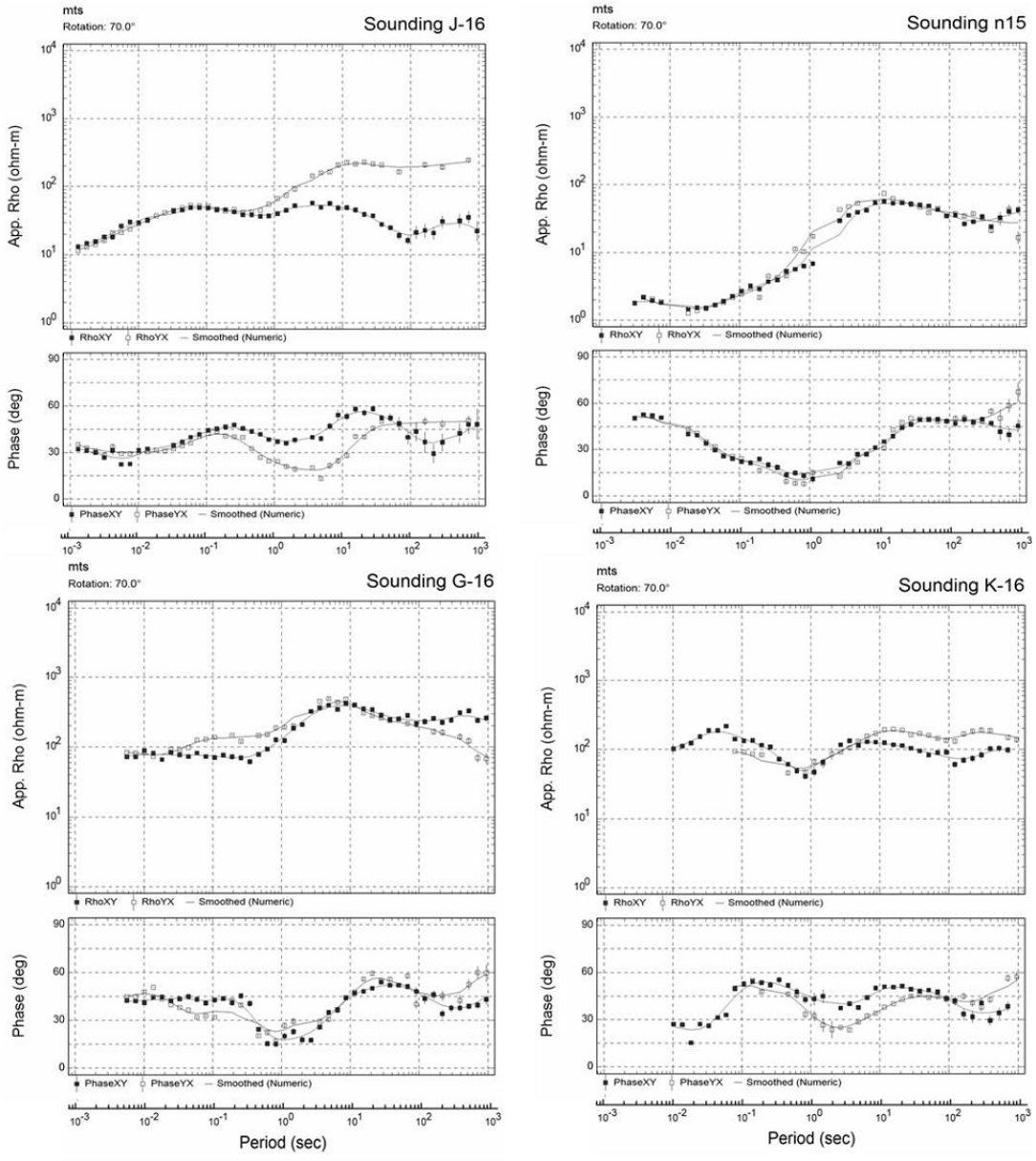

Fig.2. Typical examples of MT data in measured direction for the stations – (a) J16, N15 and (b) G16, K16.

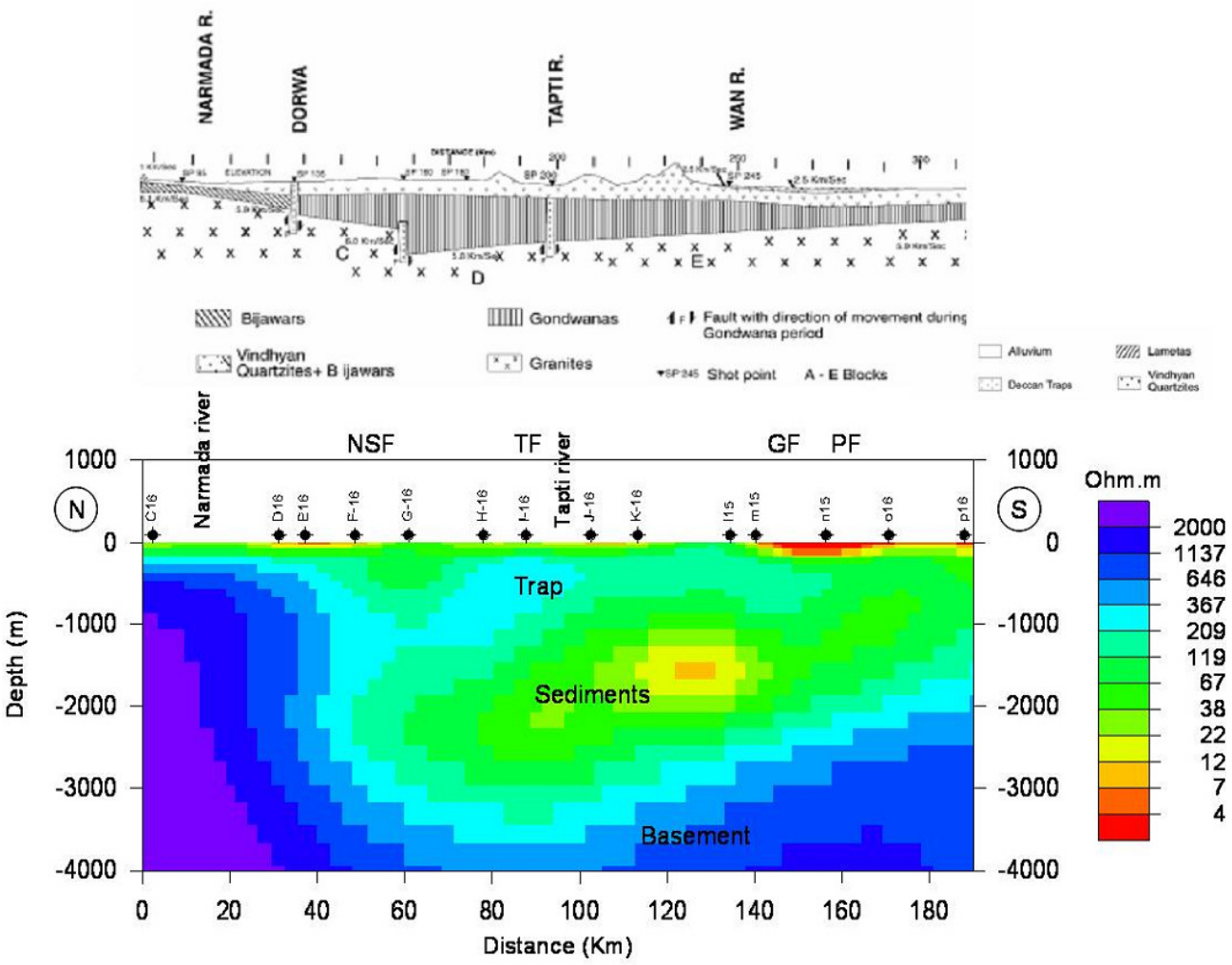

Fig.3. Shallow geoelectric section (bottom) with interpreted geological formations- Deccan trap, sediments and basement. Seismic shallow section (top) is also shown for the nearby seismic profile along Ujjain - Mahan (Kaila et al., 1985).

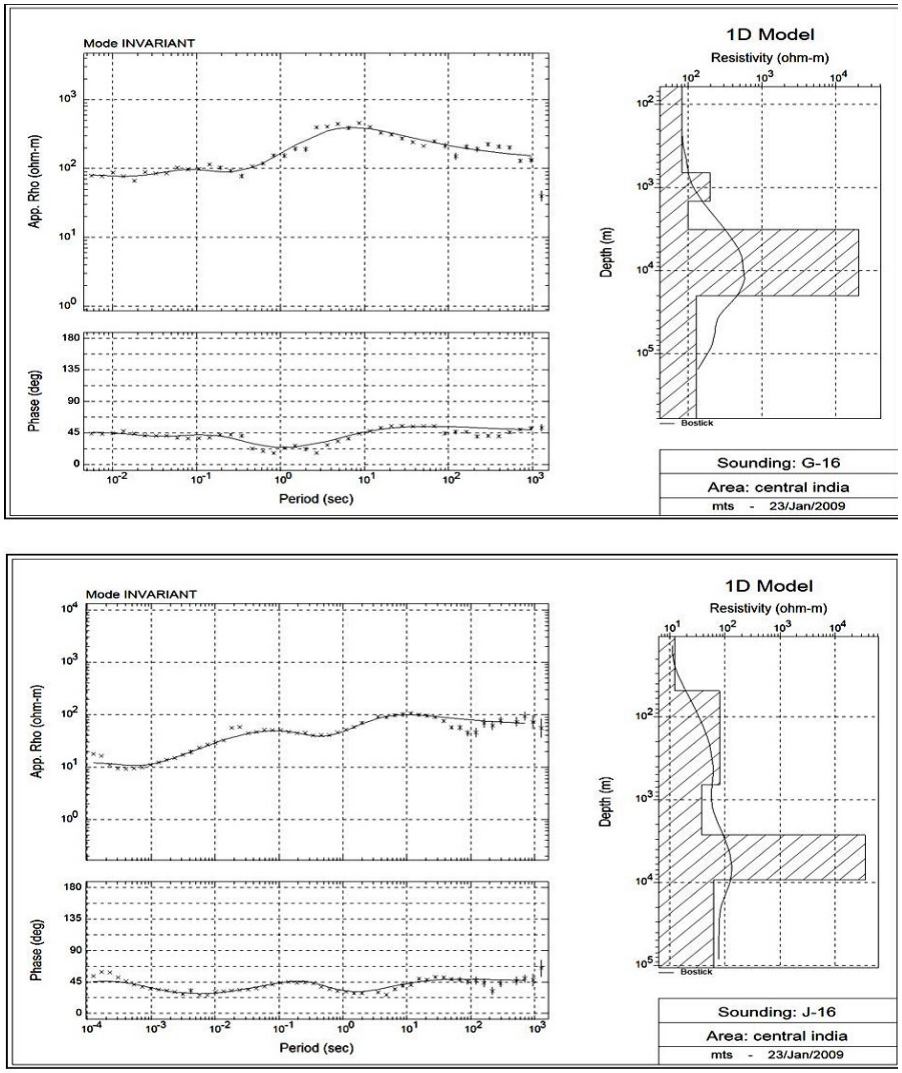

Fig. 4. For qualitative interpretation of the data, an example of Bostick 1-D modeling results for the invariant (rotationally invariant) response shows moderately resistive top layer, sediments and basement depths for the 2 stations G16, J16.